Struct Bond (2020) 185: 239–272
https://doi.org/10.1007/430_2020_74

Published online: 4 October 2020

# Time-Resolved Single-Crystal X-Ray Crystallography


**Paul R. Raithby**

## Contents



**Abstract** In this chapter the development of time-resolved crystallography is traced from its beginnings more than 30 years ago. The importance of being able to "watch" chemical processes as they occur rather than just being limited to three-dimensional pictures of the reactant and final product is emphasised, and time-resolved crystallography provides the opportunity to bring the dimension of time into the crystallographic experiment. The technique has evolved in time with developments in technology: synchrotron radiation, cryoscopic techniques, tuneable lasers, increased computing power and vastly improved X-ray detectors. The shorter the lifetime of the species being studied, the more complex is the experiment. The chapter focusses on the results of solid-state reactions that are activated by light, since this process does not require the addition of a reagent to the crystalline material and the single-crystalline nature of the solid may be preserved. Because of this photoactivation, time-resolved crystallography is often described as "photocrystallography".

P. R. Raithby (✉)
Department of Chemistry, University of Bath, Bath, UK
e-mail: p.r.raithby@bath.ac.uk

The initial photocrystallographic studies were carried out on molecular complexes that either underwent irreversible photoactivated processes where the conversion took hours or days. Structural snapshots were taken during the process. Materials that achieved a metastable state under photoactivation and the excited (metastable) state had a long enough lifetime for the data from the crystal to be collected and the structure solved. For systems with shorter lifetimes, the first time-resolved results were obtained for macromolecular structures, where pulsed lasers were used to pump up the short lifetime excited state species and their structures were probed by using synchronised X-ray pulses from a high-intensity source. Developments in molecular crystallography soon followed, initially with monochromatic X-ray radiation, and pump-probe techniques were used to establish the structures of photoactivated molecules with lifetimes in the micro- to millisecond range. For molecules with even shorter lifetimes in the sub-microsecond range, Laue diffraction methods (rather than using monochromatic radiation) were employed to speed up the data collections and reduce crystal damage. Future developments in time-resolved crystallography are likely to involve the use of XFELs to complete "single-shot" time-resolved diffraction studies that are already proving successful in the macromolecular crystallographic field.

**Keywords** Excited state lifetimes · Lasers · Macromolecules · Metastable states · Photochemistry · Photocrystallography · Solid-state · Synchrotron radiation · Time-resolved crystallography · XFELs · X-rays

## Abbreviations

| | |
|---|---|
| CCD | Charge coupled device |
| DFT | Density functional theory |
| ES | Excited state |
| ESRF | European Synchrotron Radiation Facility |
| EXAFS | Extended X-ray absorption fine structure |
| FWHM | Full width at half maximum |
| GS | Ground state |
| HATRX | Hadamard time-resolved crystallographic experiment |
| LIESST | Light-induced excited spin-state trapping experiment |
| PES | Photoelectron spectrum |
| RATIO | Method for collecting sequential laser-*on* and laser-*off* X-ray data |
| XAFS | X-ray absorption fine structure |
| XFEL | X-ray free-electron laser |

## 1 Introduction

Over the last century, single-crystal X-ray crystallography has developed into the optimum method for determining the molecular structure of materials in the crystalline state and, as this volume of Structure and Bonding shows, now underpins many aspects of the physical and life sciences. What the standard crystallographic method provides is a full three-dimensional picture of the structure of the starting material and of the product of the reaction if both can be obtained in a crystalline form. What it does not do is provide a pathway by which the starting material is converted into the product, and, since the reaction may not occur in the solid state, the immediate relevance to a solution or gas phase chemical reaction may not be apparent [1].

The reason for this inability to follow a solid-state chemical process is because the single-crystal X-ray crystallographic experiment is both space and time averaged. In terms of space averaging, every unit cell in the crystal contributes to the diffraction pattern obtained, so if some molecules within the crystal are changing and others are not, an average of the structures will be obtained. This is commonly observed in crystal structures when, for example, various parts of the molecule adopt different orientations in different unit cells or lattice solvent molecules adopt different orientations; this is termed disorder [2]. The crystallographic experiments are also time averaged. Although a single X-ray photon may interact with the electron cloud that surrounds an atomic nucleus in crystal in $10^{-18}$ s, it has to be remembered that in a single-crystal X-ray crystallographic experiment, the whole crystal has to be sampled. Typically, the crystal may contain $10^{15}$ molecules or more, and even with modern laboratory-based diffractometers, the sampling process takes between minutes and hours, so that the crystal structure obtained is an average over the whole duration of the data collection [3].

A further problem associated with following chemical or biological processes within a single crystal is the retention of crystallinity throughout the process since a loss of crystallinity caused by degradation of the crystal means that a single-crystal diffraction experiment is no longer viable. This limits the type of reaction that can be followed. Adding a reagent to a crystal to facilitate a chemical reaction will usually destroy the crystal, although there are an increasing number of examples, often associated with crystals of framework structure materials, where small molecules (liquids or gases) can be introduced into the crystal and can undergo a reversible or irreversible physical or chemical process [4–6]. A much easier way of facilitating a single-crystal-to-single-crystal reaction is to use an external medium such as irradiation with light [7–9], application of pressure [10–12] or change in temperature [13–15] which is less likely to disrupt the crystalline lattice, and such experiments have been becoming more feasible over the last few decades because of advances in technology.

Over the last three decades, developments in synchrotron facilities, X-ray detectors, cryogenic apparatus, laser technology, computing power and data storage capacity have all enabled single-crystal X-ray studies to provide information about solid-state reactions and dynamic processes that occur in crystals. Now chemical and

biological processes that occur in crystals can be monitored in "real time", and three-dimensional structural information on species that exist in the solid state for only fractions of a second may be obtained [16–18]. Regarding the external media for inducing reactions in crystals, the use of "light" has proved the most popular and is arguably the least likely to cause crystal degradation. Photochemically induced chemical reactions are relatively easy to control. The size, shape and intensity of the incident beam can be controlled using a wide variety of optical equipment and, when using a tuneable source, the wavelength can be varied to match the process involved. This has led to the development of "photocrystallography" [19], a term attributed to Philip Coppens [20], one of the pioneers in the area, although the crystallography of photoactivated species is also included in the description of "photosalient" processes [21] or, more generally, as "time-resolved" crystallography. With all the technological developments, the speed of a full single-crystal X-ray data collection has been reduced to minutes particularly when a high-intensity synchrotron source is used. This has provided the opportunity to undertake a whole range of new crystallographic experiments that can follow the dynamics of a chemical process and obtain a full three-dimensional picture of photoactivated species. This chapter will highlight some of the technological and experimental results that have been obtained in the first 20 years of the twenty-first century.

Of all the technological advances that have facilitated the growth of photocrystallography, it is the more general availability of synchrotrons as research tools that has proved to be most important. They have been used to apply a range of analytical techniques to study chemical and biological samples by providing high-intensity electromagnetic radiation as the probe. A synchrotron is a storage ring in which electrons are accelerated around the ring at speeds approaching the speed of light and, as a consequence, are subject to relativistic effects. This causes the electrons to circulate around the ring in discrete bunches. The resultant radiation is used in different experimental stations which are at the end of beamlines radiating out tangentially from the storage ring. Some of these beamlines are dedicated to crystallographic experiments and use X-rays with wavelengths in the range 0.4–2.5 Å [22]. A schematic representation of a synchrotron ring is illustrated in Fig. 1 which shows how the electrons are initially accelerated from their source through a linear accelerator, through a booster synchrotron into the main storage ring where their circular orbits are controlled by magnetic fields and their energies are controlled by insertion devices which guide the X-ray beam to the experimental hutch where the X-ray diffractometer sits.

## 2 Photocrystallographic Methodology

The type of photocrystallographic experiment that can be carried out is dependent on the lifetime of the photoactivated species that is being studied. The lifetimes of the various processes can range from hours to femtoseconds as are summarised in Fig. 2 so that the type of experiment that can be carried out and the results that can be

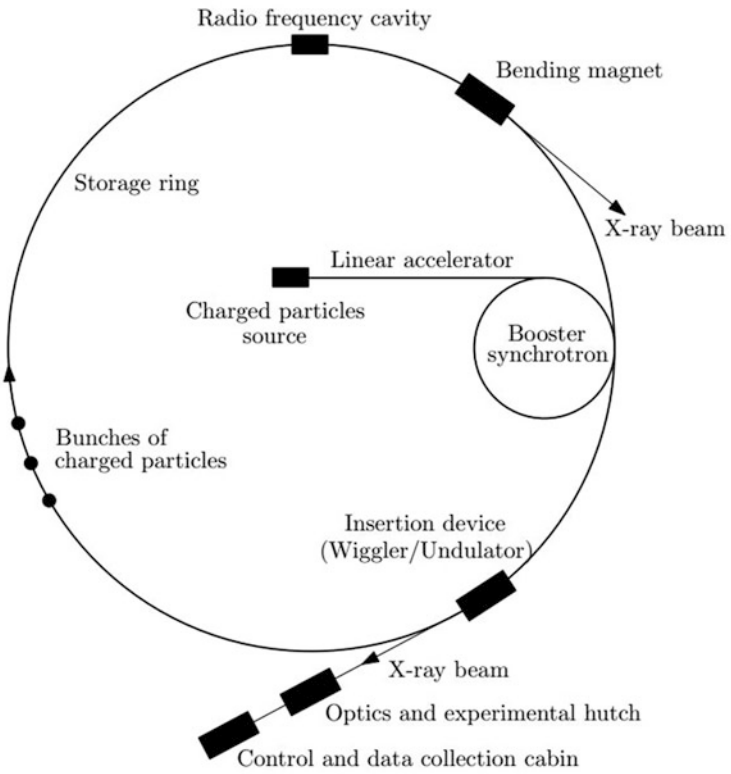


**Fig. 1** A schematic of a synchrotron ring showing a tangential beamline

obtained must be considered carefully beforehand. The photoactivated "excited state" (ES) must exist for longer than the time required for the data collection, although it can be maintained by repeatedly or continuously pumping light into the system. The experiment and the chemical process that is being studied must be brought on to a common timescale for the experiment to be successful. This can be achieved either by slowing the photoreaction down to the timeframe of the crystallographic experiment or speeding up the experiment to match the lifetime of the excited state species. The photoreaction can be slowed down by effectively using trapping strategies, e.g. chemical- or cryo-trapping methods, which involve a sudden change in the reaction conditions in order to "freeze" the reactant in a transient state for a period of time long enough to permit the analysis. While there are some advantages to this approach, the trapping process may change the natural progress of the solid-state reaction. To be sure of observing the true reaction pathway, it may be advisable to adopt the second strategy and speed up the data collection methodology so that the photoinduced process can be followed in real time.

In summary, the shorter the lifetime of the photoexcited species, the more challenging is the photocrystallographic experiment that is required to characterise

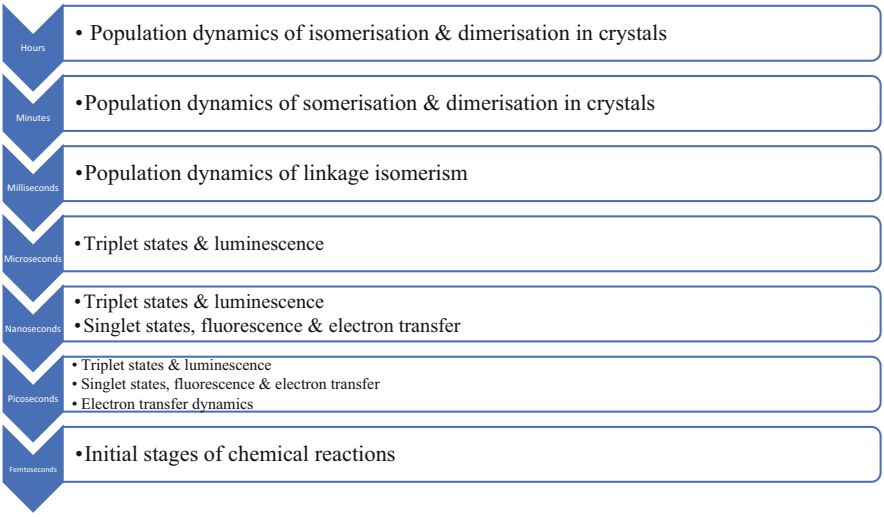


**Fig. 2** Timescales of the dynamic processes that occur in chemistry

the structure of the excited state. Photocrystallographic experiments can be characterised into three types depending on the lifetime of the excited state species.

## *2.1 Steady-State and Pseudo-Steady-State Methodologies*

At longer timescales, from milliseconds upwards, "steady-state" or "pseudo-steady-state" experiments can be carried out using standard single-crystal X-ray diffraction methods [8, 18, 23] with monochromated X-ray radiation. The steady-state methodology is used typically to study metastable excited states, those with lifetimes of hours up to infinity, if the excited state is generated and maintained at the appropriate low temperature [24]. The metastable state is generated, at a given temperature, by irradiating the sample for a period long enough to maximise the conversion from the ground state. The irradiation is then stopped, and a standard single-crystal X-ray data collection is performed. Under these experimental conditions, there are no concerns about sample heating from the irradiation source since this has been switched off prior to the start of the data collection. This process is illustrated in Fig. 3a where the ground state, unexcited structure is collected first (in order to provide a benchmark against which changes in the photogenerated excited state can be compared), then the excited state is generated with light irradiation and finally the structure is redetermined using X-rays, the light source having been turned off. Pseudo-steady-state methodology is used to study samples with slightly shorter excited state lifetimes, usually in the range of milliseconds to minutes. In these experiments the

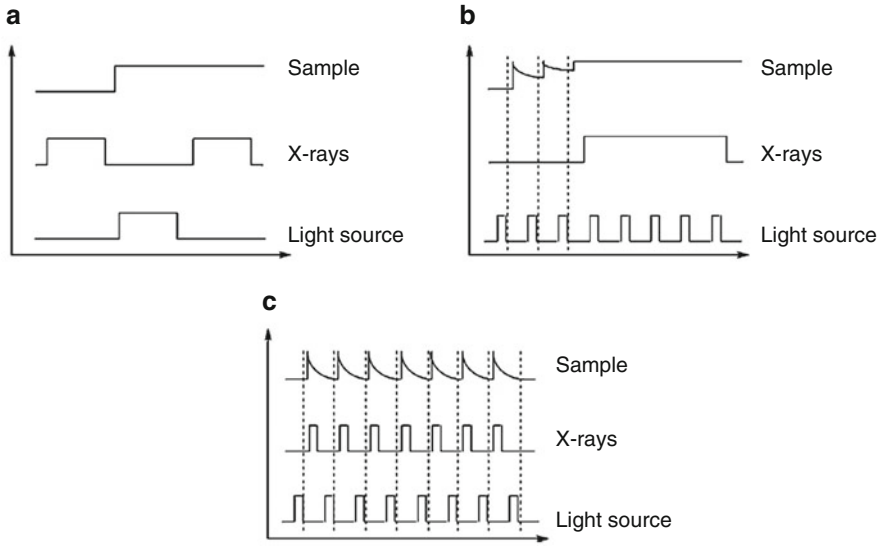


**Fig. 3** Schematic diagrams to show the timing sequences used in the different types of photocrystallographic experiments: (**a**) steady-state methods, (**b**) pseudo-steady-state methods and (**c**) pump-probe methods. *Taken from Ref.* [18] *with permission from Elsevier*

crystalline sample is irradiated throughout the data collection to maintain a constant excited state occupancy, as illustrated in Fig. 3b. This shows the excited state being pumped up to a "steady state" with repeated pulses of light before the X-ray data collection commences, the excited state being maintained throughout the data collection by continued pulses of light. Thus, this method requires an effective means of illuminating the crystal fully throughout the data collection without the movement of the diffractometer blocking the illumination source at any point. Since the sample is irradiated throughout the experiment, heating effects at the sample resulting from the irradiation source may result and have to be mitigated.

## *2.2 Stroboscopic or Pump-Probe Methodologies*

In order to study transient photoinduced species, with lifetimes of microseconds and below, "stroboscopic" or "pump-probe" photocrystallographic methods are required as shown in Fig. 3c, the sample being repeatedly re-excited and only probed by the X-rays when in the excited state. The experiments generally require short-duration light and monochromatic X-ray pulses to be generated that are synchronised to arrive at the sample position in a specific time sequence [25] or to use a time-gated detector which is synchronised with the light pulses [26] so that X-ray data is only recorded when the crystal is activated. The light source for these experiments is usually a

pulsed laser that generates pulses on the nanosecond or picosecond timescale. The X-ray source can be pulsed in a number of ways. Initially, for experiments involving crystalline species with lifetimes in the nanosecond to microsecond range, the X-ray pulses were generated by placing a mechanical chopper in the incident beam [25, 27] which interrupts the beam so that the X-rays are only "on" in synchronisation with the laser pulse. When using these short pulses, the X-ray flux that impinges on the crystal is limited, and in order to overcome this problem, high-intensity synchrotron radiation is normally required. Even with this higher X-ray intensity, many pump-probe laser and X-ray cycles are required per data collection frame to build up a sufficiently strong diffraction image, and many frames are required in order to obtain a complete X-ray data set. The repeated pumping and probing usually has a detrimental effect on the crystalline sample, and significant sample heating effects may also be a problem.

One development to overcome the crystal degradation problem has been devised and used effectively in the macromolecular crystallographic community, and that is the pump-multi-probe method based on the Hadamard transformation [28]. In the conventional pump-probe approach described above, the photoactivation event is initiated by a laser pulse and then probed at a later time by an X-ray pulse, so that every laser (pump) pulse is followed by a single probe (X-ray) pulse after a predetermined time delay (see Fig. 4a). Therefore, to measure $n$ time points, $n$ pump-probe pairs are required. In contrast, in the Hadamard approach, each pump pulse is followed by a sequence of probe pulses, and the total signal from each sequence is recorded in a single measurement (see Fig. 4b). The sensitivity of the experiment is thus defined by the total number of photons in the complete probe sequence, with the time resolution defined as the total probe sequence length divided by the number of pulses. This method no longer limits the time resolution that can be achieved to the brilliance of the X-ray source by summing the time points across the probe sequence. It also gives an improved signal-to-noise ratio because of the larger number of photons recorded during the measurement.

As in standard pump-probe experiments, $n$ pump-probe sequences are required to measure $n$ time points. The pattern of the probe sequence is represented as rows of a $n$x$n$ matrix (S) obtained from the Hadamard sequence. The simplest case is shown in Fig. 4b where each row of the matrix (and the probe sequence) is obtained by cycling by one element from the previous row to the left (see Fig. 4c).

For the Hadamard time-resolved experiment, the photoactivation is initiated and then the complete probe sequence (first row of the **S** matrix) is recorded as a single image. This process is repeated on the sample after relaxation but with the probe sequence now defined by the second row of the **S** matrix, until all the rows have been completed. The resulting encoded signals from the $n$ excitations are then collated to form a vector **W** of length $n$. The time-dependent signal, $I_t$, is then obtained by reversing the probe sequence encoding by multiplying the vector W by the inverse of the matrix **S**, so that $I_t = \mathbf{S^{-1}W}$. A time-resolved crystallographic Hadamard experiment has been dubbed a HATRX experiment.

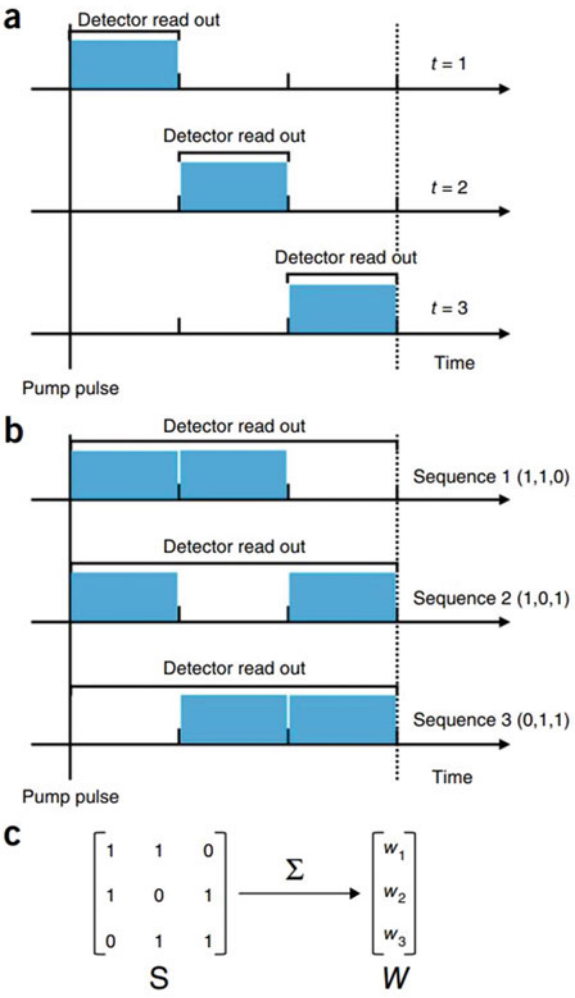


**Fig. 4** (**a**) The time sequence for the classical pump-probe method showing three time delays. (**b**) The simplest Hadamard pulse sequence set up to measure three time points. (**c**) The 3 × 3 Hadamard **S** matrix showing how each row produces a single summed intensity for each reflection on the detector ($w_1$, . . ., $w_n$) forming the vector **W**. *Figure reproduced from Ref.* [28] *with permission from Nature Methods*

## *2.3 Laue Methods*

The time-resolved experiments described so far have used monochromatic X-ray radiation. An alternative way of overcoming the limited flux in short-duration time-resolved crystallographic experiments is to change from monochromatic radiation to the Laue method where polychromatic X-ray radiation is used [29, 30]. The main advantage of the Laue method is the broader energy range used, compared with the narrow beam from a monochromator. This results in a substantial increase in intensity. The method used in both molecular [31] and macromolecular [32] crystallographic experiments is often called the pink-Laue method as "pink" indicates quite a small range of wavelengths as opposed to all the wavelengths available in the

full “white” beam. The pink-Laue method eliminates the need for the thousands of pump-probe cycles required in the stroboscopic method used for monochromatic data sets [33]. Because of the reduced time for the experiment, the crystal deterioration caused by laser and X-ray exposure may be reduced and the heating caused by the repeated laser pulses may also be reduced. In the best possible case, a single synchrotron pulse is sufficient to record a good enough diffraction pattern to solve the crystal structure [34]. In other examples several pump-probe cycles are required before a sufficiently intense diffraction pattern is obtained.

For pink-Laue data, a wavelength dependence correction has to be applied to the intensity data, because diffraction spots are being obtained from many wavelengths, and there also has to be a fitting of intensities of equivalent reflections that appear. With molecular crystals having relatively small unit cells, this scaling of intensities is challenging because there are relatively few of them. To avoid this difficulty, the RATIO method can be used [35], a method that will be explained in further detail below. A second complication with pink-Laue data is that there is a steep slope of wavelength distribution on the high-energy side of the pink-Laue spectrum. A small change in the unit cell dimensions on exposure, as would be expected with excitation, might lead to anomalous values of the *on/off* ratios of reflections scattered by wavelengths in this narrow region. The effect would be small if the conversion percentage from the ground to the excited state is small and also if the temperature increase is small. The affected reflections can be identified in the analysis of equivalent reflections and confirmed by checking the calculated wavelength from the Bragg angle and the *hkl* index after indexing. These can be removed from the averaging procedures and used to establish the structural changes that have taken place in the excited state.

As indicated above, the most sensitive measure of the structural change in a crystal when it is photoactivated into an excited state is the observed change in intensity of each of the reflections. In the RATIO method [35], this intensity difference is identified by using the *on/off* ratios as the observables in the activated structure refinement program LASER [36]. As explained in the previous paragraph, the advantage of the RATIO method when used in a Laue data collection is the elimination of the need to have a spectral curve to determine the wavelength at which each reflection is observed. To exploit the method, the laser-*on* and laser-*off* intensities for each reflection need to be collected immediately after one another. This eliminates variations in the intensity of the X-ray beam over time. This, in turn, adds an error to the intensity of the individual reflections and also eliminates the effect of any slow deterioration of the crystalline sample. In addition, slight differences in the absorption correction may occur if the laser-*on* and laser-*off* reflections were collected at different times in different settings. Finally, scaling is not required as the paired frames are collected at the same temperature and under the same conditions.

Even with these advances, it is often necessary to use multiple crystals of a crystalline sample, because of crystal deterioration, in order to obtain a complete data set. Scaling of the data sets is then required before electron density maps can be calculated and the structure solved and refined. Various scaling methods have been

applied from the simplest form which is based on the fractional change of each of the reflections on exposure to light to more sophisticated weighted least-squares scaling [31, 37].

Once the Laue data has been collected and the data set corrected, as with monochromatic photocrystallographic experiments, it is usual to compute a Fourier photodifference map to evaluate the structural changes that occur upon photoexcitation [38]. When using the RATIO method, the photodifference Fourier map is simply based on the difference between the observed laser-*on* and laser-*off* structure factors [29, 39]. These calculations are based on the fact that the crystal does not change phase (crystal system or space group) upon excitation which is generally true because percentage conversions from ground to excited state structures upon excitation are low for the short-lived species generated.

In an alternative approach to the pump-probe experiments, rather than synchronising the laser pump pulses with X-ray probe pulses generated by use of a mechanical chopper, new detector technology has allowed the X-ray detector to be synchronised with the laser pulse so that the detector only records X-ray intensity while the laser is on (or records after a designated time delay). These new detectors have fast read-out times, have the ability to internally stack series of recorded images and, most importantly, provide very fast and reliable "gating" affording fine control of when the detector is recording or not. With the efficiency of these detectors, some of the limitations of the X-ray flux can be minimised, and it is possible to consider the use of laboratory X-ray sources instead of synchrotrons for some longer lifetime photocrystallographic experiments. The use of a gated hybrid pixel detector, mounted on a conventional laboratory X-ray diffractometer, has been proven in an analysis of the photoinduced linkage isomerism of sodium nitroprusside [26]. The light-induced intensity variation between ground and excited states was detected at the 1% level, caused by the photoswitching of the nitrosyl group, and this change could be detected in a 6 microsecond window. The experimental approach is illustrated in Fig. 5. In the experiment a continuous X-ray beam impinges on the sample, and during the pump-probe cycle, with the structure continuously changing, the scattered diffraction pattern is sampled by the gated detector. The X-ray signal is only detected during a short adjustable window $X(t)$. The laser pulse serves as a trigger for the gating of the detector and synchronisation with a tuneable time delay $\Delta t$. The maximum time resolution possible is also dependent on the electronic response time of the X-ray detector.

With the gated hybrid pixel detector, the photon counting statistics determine the quality of the data, and there is no dark current or read-out noise as with a conventional CCD detector. The signal acquisition is defined by a tuneable measurement time window ($X(t)$ in Fig. 5) whose temporal width is only limited by the detector response time, which is the order of 100–200 ns. Also, with the pixel detector, it is possible to have a number of simultaneous measurement windows, with different delay times that can be acquired by the detector at the same time. This means that multiple time-resolved experiments could be carried out at the same time.

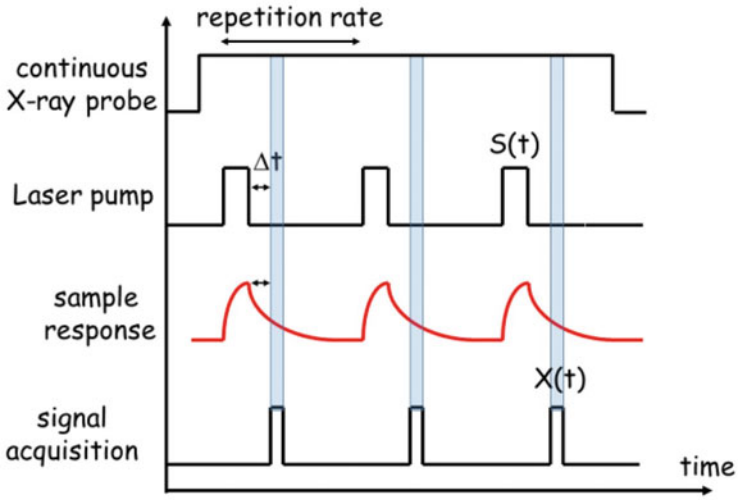


**Fig. 5** A continuous X-ray beam with a scattered signal sampled by a fast-gated detector (only one delay time shown). *The figure is reproduced from Ref.* [26] *with permission from the IUCr*

## *2.4 Sub-picosecond and XFEL Methodologies*

The interest in studying chemical and biological processes with shorter and shorter lifetimes using time-resolved crystallographic techniques continues to grow as technological advances make the picosecond and sub-picosecond time regimes accessible. The structure of the synchrotron beam itself can help with these developments. The relativistic effects on the electrons circulating the storage ring at speeds approaching that of light mean that they orbit the ring in discrete bunches [22]. Thus, the synchrotron radiation produced is naturally pulsed with a repetition rate that is determined by the period of the electron orbit around the ring. For third-generation synchrotrons, this is typically in the nanosecond to picosecond time regime. Therefore, pump-probe time-resolved experiments on species with lifetimes within this timeframe can be carried out without the need for a mechanical or electronic shutter to pulse the X-rays, and the laser repetition rate is synchronised with the repetition rate of the storage ring [40].

In order to cover all dynamic chemical processes, the ultimate aim must be to use photocrystallographic methods to investigate the initial stages of a chemical reaction that occur on femtosecond timescales [41]. The study of species with sub-picosecond lifetimes requires the development of "single-shot" diffraction methods where the whole diffraction pattern of the crystal is obtained in one X-ray pulse. Here the flux of the X-ray pulse needs to be extremely high in order to achieve a measurable pattern. Laue techniques provide sufficient flux to obtain the result, but the development of X-ray free-electron lasers (XFELs) with several orders of magnitude more flux than the most powerful synchrotrons is the obvious tool to

use to achieve this goal. The "diffract-and-destroy" approach has been developed at XFELs to study macromolecular systems [42–45]. From these and related studies, it is apparent that the direction-controlling, initial stages of a chemical reaction appear at timescales faster than are accessible through the use of synchrotrons which effectively have a 100 ps limit. The volume of data that is collected in one of these studies is enormous. For example, in the study of the initial stages of the photoexcitation of the photoactive yellow protein (PYP), which is triggered by the *trans-cis* isomerisation of the coumarin chromophore, $2.5 \times 10^6$ snapshots were recorded to 1.6 Å [46]. With these advances, and with the large number of data sets being collected accurate scaling between these data sets is required to obtain reliable results. It has been found from scaling analyses that the anisotropy of absorption following sample excitation can be pronounced and depends on the orientation of the crystals in the laser beam [47] so that this factor has to be taken into consideration if accurate analysis of molecular samples is to be achieved in the future.

## 3 The Beginnings of Time-Resolved Crystallography

### *3.1 Macromolecular Photocrystallography*

The initial developments in time-resolved crystallography came in the area of macromolecular crystallography because of the interest in important biological processes. These studies required faster data collection and processing techniques than had been standard. Biological crystals are also prone to decomposition particularly as a result of X-ray radiation damage, so the use of Laue methods could achieve faster data collection with less crystal decay.

The first nanosecond time-resolved macromolecular crystallographic study using Laue techniques, with a broad range of wavelengths (white beam), was reported in 1996 when Moffat and co-workers reported a study of the photodissociation mechanism of carbon monoxide in carbon monoxy-myoglobin (MbCO) [48]. The MbCO system had previously been studied in depth by ultra-fast spectroscopic techniques, and, as a result, the photoactivity of the complex in solution had been established [49–51]. In the experiments carried out at the European Synchrotron Radiation Facility (ESRF), Moffat et al. employed a pump-probe strategy consisting of an initial 7.5 nm-wide laser pump pulse at $\lambda = 630$ nm, followed by an X-ray probe pulse timed to arrive after a specific delay ($\tau$). This delay was varied so that six different data sets were completed at intervals of between $\tau = 4$ ns and 1.9 ms. The analysis of the data from the 4 ns and 1 μs data sets showed that regions of negative electron density appeared where the coordinated CO molecule had been. These observations confirmed the results of the earlier solution-based spectroscopic studies that photolysis of the Fe–CO bond had occurred and indicated that a similar occurs in the single crystal. The crystallographic data also showed a region of positive electron density below the heme centre, suggesting that the iron atom moves out of the heme plane as a result of the Fe–CO bond cleavage. This is consistent with the CO group

having dissociated from the iron and moved away from its binding position. The data sets collected with longer delays of above 1 μm did not show these electron density features, which is consistent with the CO recombining with the heme unit and the whole system re-relaxing back to the ground state, the whole process being completed within a few milliseconds. In a subsequent study, by the same research team, in 2001, further data sets were obtained with time delays of between 1 ns and 1 μm, and analysis of these data showed the position of transient docking sites within the heme pocket in which the photodisassociated CO sat [52]. The relative positions of these docking sites provided information on the photodissociation process and kinetic data describing the ligand recombination process.

The success of this time-resolved approach in establishing the pathways of biological processes led to further ground-breaking studies of proteins in photoactivated states with lifetimes down to hundreds of picoseconds [53, 54]. Using these pioneering techniques, it has proved possible to construct "molecular movies" that describe the full biological process in three dimensions [55].

While macromolecular time-resolved crystallography is not the focus of this chapter, the research area has continued to lead the discipline in terms of innovation taking full advantage of developments of, initially, synchrotron facilities [56–58] and, more recently, of the power of the XFELs [59–64]. The molecular crystallographers have much to learn from their macromolecular colleagues not least in the area of the treatment of crystal damage in high-intensity X-ray beams [65–67] and in the adaption of multi-crystal data collection techniques [68].

## *3.2 Molecular Photocrystallography*

Research into photoactivated changes in single crystals of molecular compounds commenced in the 1960s when Schmidt and Cohen reported that a series of *trans*-cinnamic acid derivatives underwent irreversible [2 + 2] photodimerization cycloaddition reactions in the solid state [69–71]. In these pioneering studies, the authors highlighted the importance of the surrounding crystalline environment on the pathway of the photodimerization reaction. They presented a series of key criteria that needed to be satisfied if a single-crystal-to-single-crystal transformation was to take place without significant crystal deterioration. These criteria were generalised in the *Topochemical Postulate*, stating that the photoreaction will follow a minimum energy pathway that imparts the lowest level of steric strain to the surrounding crystal environment. This meant that only transformations that proceeded *topotactically*, that is, with the minimum amount of movement at the atomic level could occur without crystal decay. Some subsequent improvements have been made [72] and several exceptions found [73], but the *Topochemical Postulate* remains an effective guide in the design of systems that undergo high levels of photoactivated [2 + 2] cycloaddition. More recently, crystal engineering techniques have been applied to the design of systems [73] that readily undergo photoactivated [2 + 2] cycloaddition reactions in the solid state, but the basis of the *Postulate* remains

largely intact. The crystal engineering methodologies applied to the design of monomers with suitable separations and orientations have included templating methods using both metal ions and hydrogen bonds and co-crystallisations and host-guest chemistry. Because the solid-state [2 + 2] cycloaddition process is irreversible, diffraction data can be collected at various stages throughout the reaction simply by pausing the irradiation at convenient intervals. Solid-state kinetic data has been obtained in this way on cycloaddition reactions by following the photoreaction as a function of irradiation time using single-crystal X-ray diffraction methods [74–76].

Irreversible solid-state photoreactions permit the full three-dimensional structures of the starting material and of the product to be determined using conventional single-crystal X-ray crystallographic methods as long as crystal integrity is maintained throughout the process. However, for reversible dynamic processes in the solid state, effectively snapshots of the structures in their excited states must be obtained, taking into account the lifetime of the activated species. Over the last four decades, the importance of fully reversible photoactivated processes has been realised because of their application in real-world technologies [77], including sensors, read-write data storage media, non-linear optics [78], molecular switches, amphidynamic materials [77] and molecular actuators [79–81]. Examples of reversible photochemical processes include metal-metal bond-length changes [82, 83], linkage isomerisation processes [8, 23, 84, 85] and light-induced spin-state trapping behaviour [13]. The photocrystallographic studies have established that the structural changes can be promoted and controlled in the solid state, with the concomitant control over physical properties such as colour [86, 87], luminescence [8, 17, 24, 86, 87] and refractive index [88–90].

Steady-state and pseudo-steady-state photocrystallographic techniques have been used to identify metastable species with much of the research focussing on the identification of metastable linkage isomers and on the products of light-induced excited spin-state trapping (LIESST) experiments. This work is covered in previous chapter of this book by Skelton et al. and will not be discussed in detail here other than to give a brief outline of the overall findings that can be related to the faster time-resolved photocrystallographic experiments that will be described in the next section.

The majority of photocrystallographic studies of transition metal complexes that undergo linkage isomerism under photoactivation have focussed on nitrosyl [91–94], sulphur dioxide [17, 85, 95] and nitro complexes [8]. Some general conclusions as to the processes involved can be drawn from these studies. In all cases the percentage of conversion obtained and the isomer formed are highly dependent on the wavelength of light used and the temperature at which the experiment is carried out. For a single-crystal-to-single-crystal process to occur, there is no change in the crystal system and the unit cell parameters do not change by more than 2%. There is a temperature at which the metastable limit is reached above which the excited state has a finite lifetime before returning to the ground state. The interconversion is also dependent on the flexibility of the crystal lattice and on the steric and electronic environment of the ambidentate ligand and the metal centre, as evidenced by only small changes in cell volume being observed. There needs to be sufficient space in

the lattice for the ligand to switch between one form and the other, and intermolecular interactions should either not be particularly strong or be flexible perhaps through a change in temperature [88, 96]. The accessible volume within the lattice and the flexibility of the lattice under experimental conditions relates back to the concept of the *reaction cavity* first proposed by Cohen [72] and then exemplified by Ohashi who showed subsequently that the *reaction cavity* could flex during the course of the reaction and that changes in temperature could significantly affect the process [97]. For example, lowering the temperature would cause lattice contraction, reducing the cavity size, and might thus "switch off" the reaction.

Light-induced excited spin-state trapping (LIESST) studies map the low spin-high spin interconversions in transition metal complexes with $d^4$-$d^7$ electronic configurations. The spin crossover phenomenon, with the associated change in magnetic properties, is usually activated thermally with the high spin (HS) to low spin (LS) interconversion occurring on cooling the complex to below some critical temperature. A significant number of these complexes can then undergo a photoactivated conversion from the LS state to a metastable HS state, via a long-lived triplet excited state. The photoinduced phenomenon was first identified in a study of $[Fe(1\text{-ptopyltetrazole})_6][BF_4]_2$ using Mössbauer spectroscopy [98]. The phenomenon is observable in both solution and in the solid state.

Single-crystal crystallographic and powder diffraction studies of the LIESST phenomenon soon followed [99–105], taking advantage of cryoscopic advances that allowed crystals to be relatively easily cooled below liquid nitrogen temperatures; many LIESST transitions occurring below 80 K. Since the early 2000s, the topic has continued to develop with a range of techniques being used to analyse the LIESST phenomenon [13, 106]. Of additional interest are LIESST complexes that display reverse switching from their photoinduced HS state back to a low temperature LS state which is induced via both temperature changes and "reverse-LIESST" processes, involving further irradiation of the excited LIESST state with a different excitation wavelength [107]. This two-way switching using different wavelengths of light has potential applications, making these metastable state species potential candidates for photoswitchable molecular devices.

## *3.3 Time-Resolved Molecular Photocrystallographic Studies*

For successful pump-probe molecular photocrystallographic studies, a material in which the molecules can undergo a fast, fully reversible switching process is required, and there should only be a small change in unit cell dimensions during the process. The robustness of the crystal under light and X-ray radiation is of primary importance if sufficient data is to be obtained and the excited state structure solved to atomic resolution.

### 3.3.1 Studies with Monochromatic X-Ray Radiation

Pump-probe X-ray experiments on molecular species, using monochromatic radiation rather than Laue techniques, were first described in 2001. Techert et al. reported a time-resolved study of transient changes in N,N-dimethylaminonitrile (DMABN) using stroboscopic X-ray powder diffraction (XRPD) methods [108]. Photoactivation of DMABN at $\lambda = 267$ nm resulted in an ultra-fast structural change as a result of the electronic excitation, and relaxation back to the ground state occurs on the picosecond timescale. The relaxation process was structurally analysed using synchrotron radiation with the beam being chopped mechanically and synchronised with light pulses from a Ti:sapphire laser, with pump-probe delay times ranging from −240 to 1,500 ps, allowing for several data points to be collected. The reflections that showed the greatest intensity changes during the structural rearrangement were identified, and the authors followed these intensity changes with increasing delay times. The data showed a conversion level to the excited state of between 28 and 32% at short time delays, which is consistent with spectroscopic data. Refinement of the powder data using the Rietveld method showed that the relaxation occurred via a change in the inversion angle of the molecule and a rotation of the methyl group (as shown in Fig. 6), with a total structural relaxation time of 520 ps.

Coppens was among the first to take advantage of the higher intensity of synchrotron X-ray radiation and in 2002 reported the first single-crystal X-ray diffraction study of a species with a microsecond lifetime. The results of pump-probe experiments on salts of the $[Pt_2(pop)_4]^{4-}$ anion (pop = $[H_2P_2O_5]^{2-}$) showed that structural distortions in the anion are induced by photoactivation with 355 nm light, producing a triplet excited state with a microsecond lifetime [83]. The key change in the structure upon excitation was the shortening of the Pt–Pt bond which has previously been proposed from electronic [109] and Raman spectroscopy [110] and XAFS [111] studies, the latter suggesting a reduction in Pt–Pt bond length of 0.52 Å. The pump-probe time-resolved single-crystal X-ray study was carried out on the tetra-tetraethylammonium salt of $[Pt_2(pop)_4]^{4-}$ at a temperature of 17 K and 33 μs wide light pulses from a Nd/YAG laser, at a repetition rate of 5,100 Hz, and using the "*light-on/light-off*" data collection strategy. Analysis of the excited state data showed a 2% level of excitation under the experimental conditions. Upon refinement of the Pt positions, the rest of the structure being treated as a rigid group, the Pt–Pt distance was found to shorten by 0.28(9) Å with a concomitant rotation of 3° about the Pt–Pt vector. The Pt–Pt distance has subsequently been confirmed by a second diffraction experiment [112] on the related salt $(n\text{-}Bu_4N)_2H_2[Pt_2(pop)_4]$ where the Pt–Pt reduction in length was recorded at 0.23 Å. More recently, further confirmation has come from scattering measurements of an aqueous solution [113] and a time-resolved EXAFS study [114] that showed the reduction in Pt–Pt distance from that found in the ground state structure were 0.24 Å and 0.31 Å, respectively.

Another substantial reduction in metal-metal bond length was reported for the Rh–Rh bond length in $[Rh_2(dimen)_4][PF_6]_2$.MeCN (dimen = 1,8-diisocyanomethane)

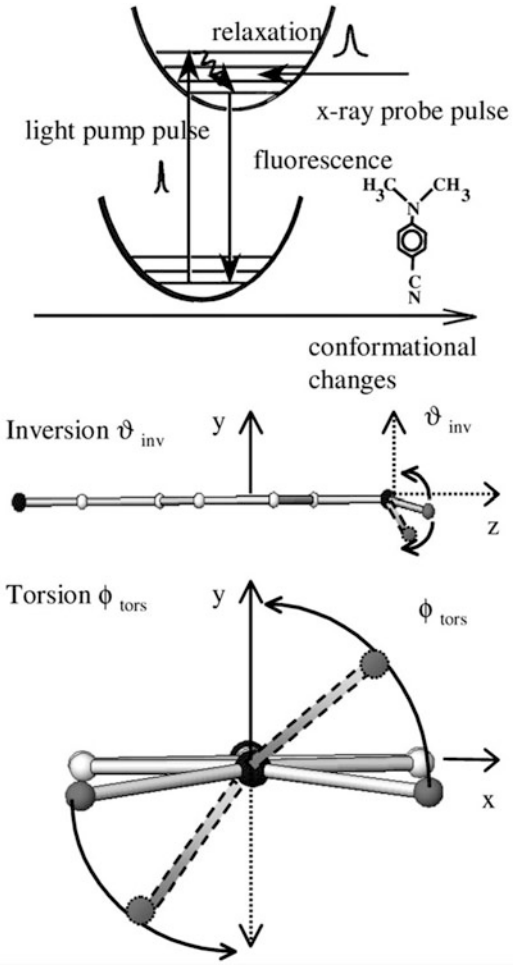


**Fig. 6** Top: The principle of TR X-ray diffraction on the excited state PES of DMABN crystals. Bottom: the intramolecular degrees of freedom, which contribute to the relaxation process (inversion qinv and torsion ftors). C atoms of the phenyl moiety are given as open, N atoms as black and the amino C as grey circles. Note that the H atoms are not shown, since they do not contribute to the X-ray diffraction signal. *Reproduced from Ref.* [108] *with permission from the ACS*

upon photoactivation at 23 K using 335 nm laser pulses. The maximum level of excitation reached was 2.5%, and the Rh–Rh bond length reduction was a remarkable 0.86 Å and a bond rotation of ca. 13° [82]. Previous spectroscopic studies on the cation had indicated a lifetime of ca. 11 μs for the triplet excited state species [115] which is in excellent agreement with the experimental value of 11.7 μs at 23 K. DFT calculations conducted at the same time as the photocrystallography experiment proposed a slightly greater decrease in the Rh–Rh distance upon excitation as illustrated in Fig. 7. The difference between the experimental and theoretical results may indicate that the steric effects from the crystalline environment may modify the structural response to the excitation process.

Further photocrystallographic studies employing stroboscopic methods were reported by Coppens et al. including an investigation of photoinduced structural

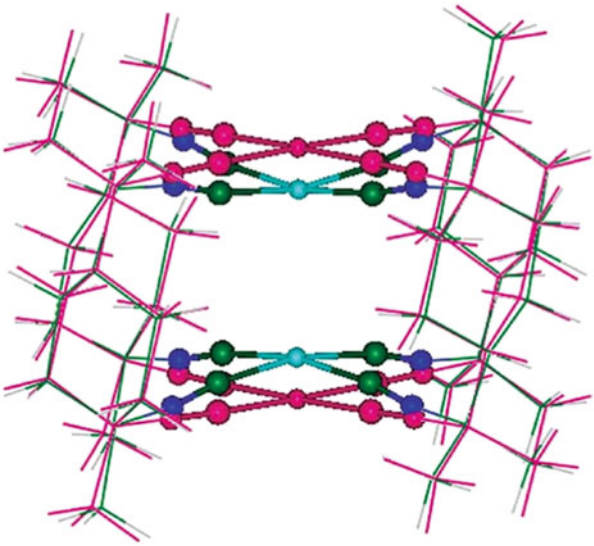

**Fig. 7** Theoretical ground state (in pink) and excited state (green and blue colours) geometries of the $[Rh_2(1,8\text{-diisocyanomenthane})_4]^{2+}$ cation. *Reproduced from Ref.* [82] *with permission from the Royal Society of Chemistry*

changes in the trimeric complex $[Cu_3(3,5\text{-}(CF_3)_2\text{pyrazolate})_3]$ [116]. This system differs from the examples discussed above because the photoexcitation occurs intermolecularly between two neighbouring copper trimer molecules, as opposed to the intramolecular processes in the di-nuclear species. Photoactivation at $\lambda = 355$ nm and 17 K promotes the production of excited state species with microsecond lifetimes, involving a rearrangement of the trimer molecules into pairs such that one inter-planar Cu...Cu distance is reduced by 0.65 Å while the next Cu...Cu contact lengthens by ca. 0.30 Å. In a separate study, conducted in 2009, significant structural distortions in the complex $[Cu(dmp)(dppe)](PF_6)$, (dmp = 2,9-dimethyl-1,10-phenanthroline) are described [117]. The complex crystallises with two, crystallographically independent molecules in the asymmetric unit, whose structural response on photoactivation is interestingly different. These differences have been attributed to different constraining effects from the surrounding crystalline environment for each of the independent molecules. In general, upon irradiation the Cu cation is observed to "flatten out", and a concomitant increase in the average Cu–P bond length is observed by comparison of the diffraction data from the ground and excited states (Fig. 8). The changes are expected to be the result of charge-transfer between the dmp and dppe ligands and were determined from an excited state population of ca. 7–10% in the single crystal.

These studies highlighted the importance of the crystalline environment on the solid-state photoactivation process and confirmed the significance of the "reaction cavity" hypothesis discussed earlier [97, 118]. In order to exploit this aspect and to use it to increase the level of conversion to the excited state species, photoactive

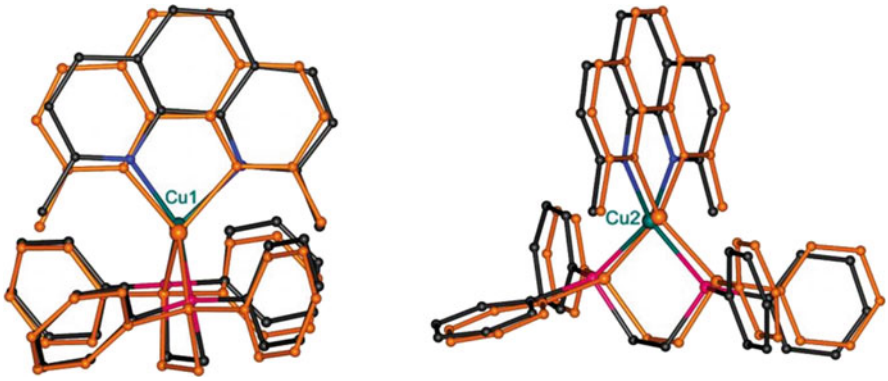


**Fig. 8** Excited state geometries of the two independent molecules (orange) superimposed on the ground state of the complex (Cu, green; C, black; P, purple; N, blue). Slightly different views are shown to illustrate the change in rocking distortion (left) and the displacement of the phenanthroline ligand from its ground state plane (molecule 2, right) upon excitation. *Reproduced from Ref.* [117] *with permission from the American Chemical Society*

complexes have been embedded as guests into arrays and framework materials. It is of importance that the host frameworks should be inert to photoactivation but effectively dilute the concentration of the photoactive species in the material. The host-guest arrangement has significant advantages for promoting the retention of crystal integrity during the process and provides greater freedom for the guest to rearrange without resulting in steric clashes with adjacent molecules in the pure material. Additionally, the dilution of the photoactive species reduces the number of photons that are required to maximise excitation, leading to more efficient photoactivation and, hopefully, increased conversion percentages [119]. It should also be noted that this approach has the effect of isolating the photoactive molecules from one another, producing quite a different environment to that experienced in crystals of the guest molecule, so differences in the physical properties of the pure compound and of the host-guest complex should be expected. Coppens et al. have investigated a number of species by this approach, via both static and dynamic photocrystallographic techniques [94, 119–121].

There have been a number of other studies using "crystal engineering" techniques involving the use of molecular cages and flasks [122] and metal organic frameworks (MOFs) to trap transient and highly reactive species [123]. Kawano et al. used synchrotron X-ray radiation to identify the coordinatively unsaturated "$\eta^5$-$(C_5H_4Me)Mn(CO)_2$" moiety in a designed self-assembled coordination cage [124]. Photoirradiation of a [$\eta^5$-$(C_5H_4Me)Mn(CO)_3$] guest molecule, within a single crystal, at 100 K, using 365 nm light, resulted in the dissociation of a carbonyl ligand remarkably without loss of crystallinity, and peaks in the electron density difference map could be attributed to free carbon monoxide. The crystallographic results were supported by a solid-state IR study. The same group has subsequently gone on to identify an unstable imine [125] and a transient hemiaminal [126], both trapped in pre-designed porous networks. They have also demonstrated the suppression of

rapid *cis-trans* isomerism in the dimeric coordination complex $[(\eta^5\text{-indenyl})Ru(CO)_2]_2$ when this molecule is trapped in a self-assembled coordination cage [127] and the conversion of an overcrowded chromic alkene to a metastable twisted conformation, upon photoactivation, when incorporated into a tetrahedrally symmetric coordination cage [128]. Champness et al. have also exploited the power of synchrotron-based X-ray crystallography to support time-resolved IR studies to probe the *fac-mer* isomerism of $[M(diimine)(CO)_3X]$ (M = Re or Mn; X = Cl or Br) units immobilised in a MOF and shown the presence of the *mer*-isomer in the photoactivated crystalline solid [129]. Subsequently, they have shown that the coordination polymer $[(Cu(DMF)(H_2O)][LRe(CO)_3Cl].DMF]_\infty$ (L = 2,2′-bipyridine-5,5′-dicarboxylic acid) undergoes an irreversible photoinduced charge transfer process. Time-resolved IR spectroscopy was used to identify the nature of this photoinduced process and how, under suitable conditions, it is possible to initiate irreversible modification of the crystal through induction of the charge transfer process. By using the photoinduced process, which arises purely as a result of the structure of the coordination network, it was possible to write on the surfaces of crystals [130].

### 3.3.2 Studies Using Laue Diffraction Techniques

Among the first time-resolved photocrystallographic studies using Laue diffraction techniques, designed to probe shorter timescales and reduce crystal damage, was carried out on a di-rhodium complex, $[Rh_2(\mu\text{-PNP})_2(PNP)_2][BPh_4]$ ($PNP = CH_3N(P(OCH_3)_2)_2$), which was studied photocrystallographically on the 100 ps timescale [29] using Laue diffraction methods. The crystal was pumped with 35 ps pulses of a Ti:sapphire laser tuned to a wavelength of 337 nm, at a temperature of 225 K, followed by a single 100 ps-wide X-ray pulse after a 100 ps delay. The lifetime of the excited state species was ca. 35 μs. In this case, the experimental results showed a shortening of the Rh–Rh distance of 0.136(8) Å upon excitation, and the results are quantitatively supported by quantum-mechanical calculations. The study shows similar, but smaller, trends to those described for $[Rh_2(dimen)_4][PF_6]_2$.MeCN above [82]. The deconvolution of the overlapping reflections was achieved during the data reduction, and the structure was refined using the RATIO method [36].

A Cu(I) complex, $[Cu(1,10\text{-phenanthroline})(PPh_3)_2][BPh_4]$, was also studied using Laue diffraction methods [131] and compared to the $[Cu(dmp)(dppe)]^+$ cation that had been studied previously using monochromatic methods [117]. This phenanthroline complex also crystallises with two independent cations in the asymmetric unit, with one molecule in a more sterically constrained environment. Photoactivation in the single crystal was expected to induce a MLCT transition, resulting in transient structural changes. The two independent molecules are again observed to undergo different structural responses upon activation with $\lambda = 390$ nm light at 90 K. Data were collected using the single-pulse Laue method, the data was analysed [132], and the results showed considerable distortion in the less restricted Cu molecule, while no significant changes were observed in the cation adopting the second, more confined arrangement (Fig. 9). Theoretical studies confirmed that the

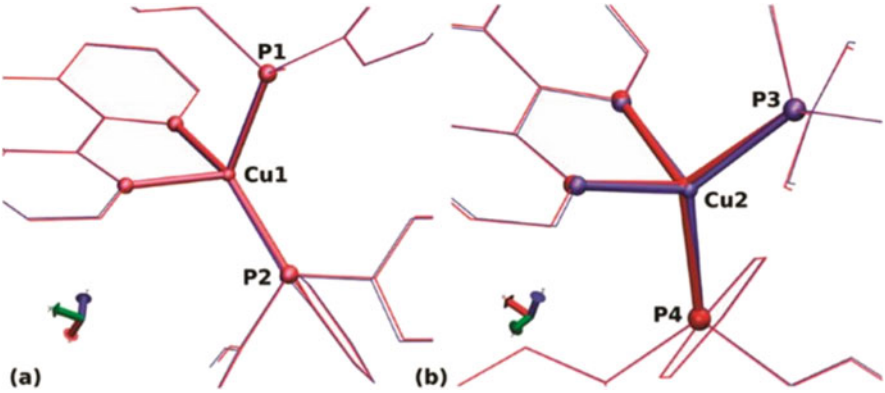


**Fig. 9** Comparison of the ground state (in blue) and the excited state (in red) structures of the two independent molecules at 90 K. (**a**) Molecule A; (**b**) molecule B. *Reproduced from Ref.* [131] *with permission from the American Chemical Society*

different responses were to be expected resulting from the interaction of the photoactive species with the surrounding lattice, with far greater distortions predicted in the free molecule than those observed experimentally in the solid state. For both this and the study on $[Rh_2(\mu\text{-}PNP)_2(PNP)_2][BPh_4]$, the experimental standard deviations for data collected by the Laue method are much improved compared to those seen with monochromatic time-resolved techniques. These improvements highlight the greater accuracy of time-resolved diffraction data collected by Laue methods for short lifetime species, which is mainly attributed to reduced levels of laser heating when adopting the single-shot approach [133].

The use of pink-beam Laue diffraction has also been applied to the time-resolved photocrystallographic study of mixed metal polynuclear complexes. The triplet excited state of the tetranuclear $d^{10}$-$d^{10}$ complex $Ag_2Cu_2L_4$ (L = 2-diphenylphosphino-3-methylindole) has been investigated with a Laue pump-probe technique with an 80 ps time resolution at 90 K [134]. The lifetime of 1 μs is accompanied by significant changes in the metal framework, with an Ag…Cu distance shortening by 0.59(3) Å, which suggests an increase in the argentophilic interactions (Fig. 10). The photocrystallographic study was accompanied by theoretical calculations which confirm that the strengthening of the Ag…Ag interaction is caused by ligand-to-metal charge transfer (LMCT).

Most recently, the luminescent properties of a tetranuclear Cu(I) benzoate complex have been investigated by a combination of time-resolved spectroscopy and crystallography. The complex $[Cu_4(PhCO_2)_4]$ displays luminescent thermochromism, with red phosphorescence at room temperature that turns green on lowering the temperature to 90 K [135]. The low-energy triplet state has been assigned to a cluster-centred triplet state, and the emission from this state matches the experimental red band observed at 660–715 nm. The computed next highest triplet excited state occurs close to the experimental value at 545 nm. The two excited states exhibit MLCT and LMCT characteristics, particularly in their solid-

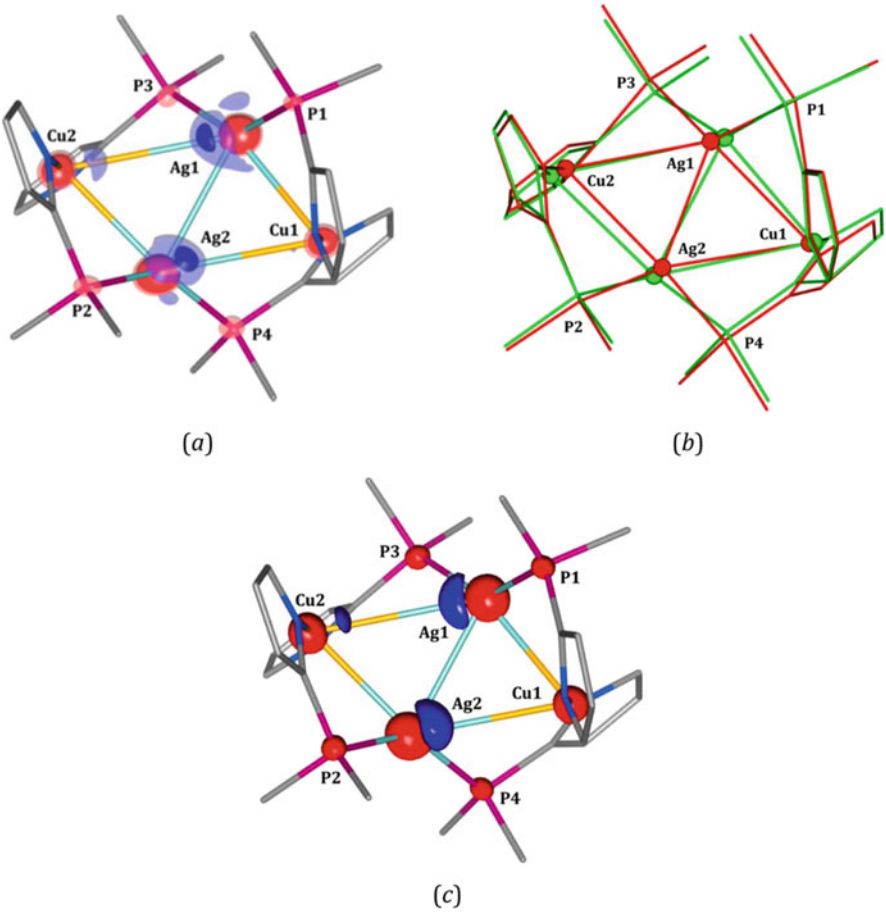


**Fig. 10** (**a**) Photodifference map ($F_o^{ON}-F_o^{OFF}$) of the complex showing atomic shifts upon excitation (solid isosurfaces, ±0.55 e·Å$^{-3}$; semi-transparent, ±0.35 e·Å$^{-3}$; blue, positive; red, negative). (**b**) Refined excited state geometry related to that of the ground state crystal structure (green, ground state; red, excited state; methylindole ligands were omitted for clarity). (**c**) Photodeformation map ($F_c^{ON}-F_c^{OFF}$) based on the refined model parameters (isosurfaces, ± 0.30 e·Å$^{-3}$; blue, positive; red, negative; $k_B = 1.06$). *Reproduced from Ref.* [134] *with permission from the American Chemical Society*

state geometries, as evidenced from the Laue photocrystallographic study, at 90 and 225 K, with 355 and 360 nm light irradiation, which shows the expected Cu. . .Cu contraction. Again, there are two independent molecules in the crystallographic asymmetric unit, and they show slightly different distortions because of their different crystalline environments.

With recent technological advances, it is not just very fast timescale photocrystallographic molecular transformations that have been carried out. It has become possible to study the dynamics of LIESST [136], and the results show

significant differences to results obtained from those of conventional diffraction studies of long-lived photoinduced high spin states. Ultra-fast spin-state photoswitching in two crystalline polymorphs of the octahedral Fe(III) complex [(TPA)Fe(TCC)] (TPA = tris(2-pyridylmethyl)amine and TCC = 3,4,5,6-tetrachloroactecholate dianion) (Fig. 11) has been studied by femtosecond optical spectroscopy and picosecond X-ray diffraction [39]. In these experiments the X-ray pulses were generated by a fast chopper, and data was collected with a series of different delay times between the laser pump and the X-ray probe. The time

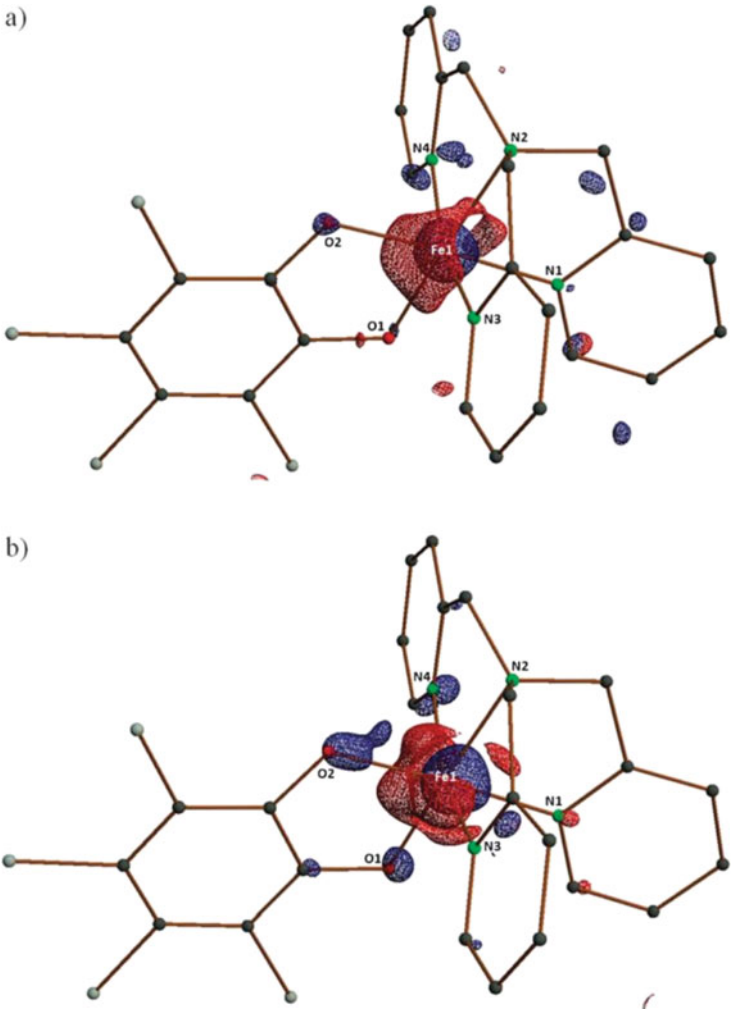


**Fig. 11** Photodifference maps obtained for the monoclinic polymorph with isosurfaces (red positive, blue negative) of (**a**) ±0.14 eÅ$^3$ for the 500 ps data and (**b**) ±0.46 eÅ$^3$ for the 50 μs data. *Reproduced from Ref.* [39] *with permission from the Royal Society of Chemistry*

dependence of the lattice parameters was measured using partial data collected for each delay time with 60 frames with 10 s of exposure for every 1° step of the diffractometer ϕ axis. Typical excitation densities were 150 $\mu m^{-2}$, with a laser diameter of ca. 500 μm (FWHM). After data processing of the full data sets for the monoclinic polymorph, photodifference maps were calculated for the 500 ps and 50 μs time delays. The maps show significant changes in electron density upon excitation (Fig. 11). The response to the excitation at 500 ps is shown by the sideways shift of electron density from the Fe1 atom towards O2 (Fig. 11a). This shift becomes even more pronounced at the 50 μs time point (Fig. 11b). There is also an increase in the Fe–N distances by ca. 0.05 Å. The estimated population of the excited state at 500 ps is in the range 1.5–2%, and this increases to ca. 10.5% after 50 μs. Overall, the results show significant shifts of the Fe atom and the two O atoms upon excitation, and the results are consistent with the complementary spectroscopy that was undertaken.

In a subsequent study of the Fe(III) spin-crossover material, [Fe(3-MeO-SalEen)$_2$][$PF_6$], the switch from LS to HS only occurs at the molecular level as clearly shown by the linear dependence of the fraction of photoswitched molecules with the excitation density as well as with the initial fraction of low spin molecules. The inter-system crossing from the photoexcited LS (S = 1/2) to HS (S = 5/2) occurs within approximately 200 fs and is accompanied by coherent non-equilibrium vibrational relaxation in the photoinduced HS state. These results reveal similar dynamical features to those already reported for LIESST in related Fe(II) systems [137]. The activation of coherent molecular vibrations is an essential requirement for reaching the HS potential on the timescale of molecular motions, whereas their fast damping allows an efficient trapping in the HS potential [138]. The observed coherent oscillations are attributed to photoinduced molecules in the HS states, and the results are supported by Raman spectroscopy at thermal equilibrium and DFT analyses of molecular vibrations and TD-DFT calculations of optical absorption.

## 4 Conclusions

Time-resolved crystallography has developed extensively over the last three decades, and the results presented in this chapter show that under favourable conditions it is possible to obtain full three-dimensional structural data on chemical species that have lifetimes of microseconds or less [139]. These advances, coupled with similar advances in instrumentation and computer power, open up possibilities for monitoring chemical processes in the solid state in a way that has not previously been possible. At present the restrictions of maintaining crystal integrity remain, and the reactions and processes are mostly limited to the interaction of the solid to external media such as light, as discussed in this chapter, but also to changes in temperature and pressure and the influence of magnetic and electric fields (although crystal integrity is retained in some solid-gas reactions). The potential is enormous,

and the topic is ripe for development. As has already been indicated, the new frontier in photocrystallography over the next several decades is the use of X-ray free-electron laser sources to carry out serial femtosecond studies [41]. The use of XFELs to track chemical reactions by serial femtosecond pump-probe X-ray crystallography by rapidly recording diffraction patterns at closely spaced time intervals has already proved successful in macromolecular crystallography [42, 43, 45]. Once the scaling issues related to using multiple crystals in serial processes are resolved and diffraction patterns better than atomic resolution [47] are obtained, the prospect for carrying out molecular crystallography at an XFEL is extremely promising.

In the meantime, for the slower timescale processes (milliseconds to minutes), detector development will facilitate the use of laboratory sources [26, 140], rather than the need for synchrotrons. This will mean that many more "routine" time-resolved experiments can be carried out and there are thousands of systems which would benefit from structural dynamic studies. Additionally, the monitoring of dynamic processes using multiple techniques simultaneously, such as the combination of photocrystallography with emission spectroscopy or Raman spectroscopy, will allow the detailed processes within the molecule as well as changes in the crystalline environment to be monitored in exquisite detail.

**Acknowledgements** PRR gratefully acknowledges the support of the Engineering and Physical Sciences Research Council (EP/K004956) and the Diamond Light Source for the provision of beamtime.

**Dedication** This chapter is dedicated to Professor Alan J. Welch of the Chemistry Department, Heriot-Watt University, Edinburgh, Scotland, on his retirement. Alan was completing his Ph.D. in Chemical Crystallography in Mike Hursthouse's research group at Queen Mary College, London, when I joined the group to start mine. Alan guided me through the first year of my Ph.D., and I am very grateful to him for passing on all his crystallographic knowledge. We have kept in touch ever since, and it is nice to have this opportunity to recognise Alan's outstanding contribution to structural chemistry.

## References

1. Burgi HB, Dunitz JD, Shefter E (1973) Geometrical reaction coordinates. II Nucleophilic addition to a carbonyl group. J Am Chem Soc 95(15):5065–5067
2. Clegg W, Blake AJ, Cole JM, Evans JSO, Main P, Parsons S, Watkin DJ (2009) Crystal structure analysis: principles and practice. Oxford University Press, Oxford. Incorporated
3. Weller MT, Mark TW (2017) Young NA, Nigel AY (eds) Characterisation methods in inorganic chemistry. Oxford University Press, Oxford
4. Naumov P, Bharadwaj PK (2015) Single-crystal-to-single-crystal transformations. CrstEngComm 17(46):8775–8775
5. Chaudhary A, Mohammad A, Mobin SM (2017) Recent advances in single-crystal-to-single-crystal transformation at the discrete molecular level. Cryst Growth Des 17(5):2893–2910
6. Bryant MJ, Skelton JM, Hatcher LE, Stubbs C, Madrid E, Pallipurath AR, Thomas LH, Woodall CH, Christensen J, Fuertes S, Robinson TP, Beavers CM, Teat SJ, Warren MR, Pradaux-Caggiano F, Walsh A, Marken F, Carbery DR, Parker SC, McKeown NB, Malpass-

Evans R, Carta M, Raithby PR (2017) A rapidly-reversible absorptive and emissive vapochromic Pt(II) pincer-based chemical sensor. Nat Commun 8
7. Lee JH, Park S, Jeoung S, Moon HR (2017) Single-crystal-to-single-crystal transformation of a coordination polymer from 2D to 3D by [2 + 2] photodimerization assisted by a coexisting flexible ligand. CrstEngComm 19(27):3719–3722
8. Hatcher LE, Skelton JM, Warren MR, Raithby PR (2019) Photocrystallographic studies on transition metal nitrito metastable linkage isomers: manipulating the metastable state. Acc Chem Res 52(4):1079–1088
9. Commins P, Desta IT, Karothu DP, Panda MK, Naumov P (2016) Crystals on the move: mechanical effects in dynamic solids. Chem Commun 52(97):13941–13954
10. Moggach SA, Parsons S (2009) High pressure crystallography of inorganic and organometallic complexes. Spectroscopic properties of inorganic and organometallic compounds. The Royal Society of Chemistry 40:324–354
11. Woodall CH, Beavers CM, Christensen J, Hatcher LE, Intissar M, Parlett A, Teat SJ, Reber C, Raithby PR (2013) Hingeless negative linear compression in the mechanochromic gold complex [(C6F5Au)2(μ-1,4-diisocyanobenzene)]. Angew Chem 125(37):9873–9876
12. Shepherd HJ, Rosa P, Vendier L, Casati N, Létard J-F, Bousseksou A, Guionneau P, Molnár G (2012) High-pressure spin-crossover in a dinuclear Fe(II) complex. Phys Chem Chem Phys 14 (15):5265–5271
13. Halcrow MA (2011) Structure:function relationships in molecular spin-crossover complexes. Chem Soc Rev 40(7):4119–4142
14. Legrand Y-M, van der Lee A, Masquelez N, Rabu P, Barboiu M (2007) Temperature induced single-crystal-to-single-crystal transformations and structure directed effects on magnetic properties. Inorg Chem 46(22):9083–9089
15. Reinoso S, Artetxe B, Gutierrez-Zorrilla JM (2018) Single-crystal-to-single-crystal transformations triggered by dehydration in polyoxometalate-based compounds. Acta Crystallogr C 74(11):1222–1242
16. Coppens P, Fomitchev DV, Carducci MD, Culp K (1998) Crystallography of molecular excited states. Transition-metal nitrosyl complexes and the study of transient species. J Chem Soc Dalton 6:865–872
17. Cole JM, Irie M (2016) Solid-state photochemistry. CrstEngComm 18(38):7175–7179
18. Hatcher LE, Raithby PR (2014) Dynamic single-crystal diffraction studies using synchrotron radiation. Coord Chem Rev 277:69–79
19. Cole JM (2008) Photocrystallography. Acta Crystallogr A 64:259–271
20. Coppens P (2009) The new photocrystallography. Angew Chem Int Ed Engl 48 (24):4280–4281
21. Naumov P, Sahoo SC, Zakharov BA, Boldyreva EV (2013) Dynamic single crystals: kinematic analysis of photoinduced crystal jumping (the photosalient effect). Angew Chem Int Ed 52(38):9990–9995
22. Clegg W (2000) Synchrotron chemical crystallography. J Chem Soc Dalton 19:3223–3232
23. Hatcher LE, Raithby PR (2013) Solid-state photochemistry of molecular photo-switchable species: the role of photocrystallographic techniques. Acta Crystallogr C 69:1448–1456
24. Hatcher LE, Skelton JM, Warren MR, Stubbs C, da Silva EL, Raithby PR (2018) Monitoring photo-induced population dynamics in metastable linkage isomer crystals: a crystallographic kinetic study of [Pd(Bu4dien)NO2]BPh4. Phys Chem Chem Phys 20(8):5874–5886
25. Fullagar WK, Wu G, Kim C, Ribaud L, Sagerman G, Coppens P (2000) Instrumentation for photocrystallographic experiments of transient species. J Synchrotron Radiat 7:229–235
26. Casaretto N, Schaniel D, Alle P, Wenger E, Parois P, Fournier B, Bendeif E, Palin C, Pillet S (2017) In-house time-resolved photocrystallography on the millisecond timescale using a gated X-ray hybrid pixel area detector. Acta Crystallogr B Struct Sci Cryst Eng Mater 73:696–707
27. Husheer SLG, Cole JM, d'Almeida T, Teat SJ (2010) A prototype chopper for synchrotron time-resolved crystallographic measurements. Rev Sci Instrum 81(4)

28. Yorke BA, Beddard GS, Owen RL, Pearson AR (2014) Time-resolved crystallography using the Hadamard transform. Nat Methods 11(11):1131–1134
29. Makal A, Trzop E, Sokolow J, Kalinowski J, Benedict J, Coppens P (2011) The development of Laue techniques for single-pulse diffraction of chemical complexes: time-resolved Laue diffraction on a binuclear rhodium metal-organic complex. Acta Crystallogr A 67:319–326
30. Schmokel MS, Kaminski R, Benedict JB, Coppens P (2010) Data scaling and temperature calibration in time-resolved photocrystallographic experiments. Acta Crystallogr A 66:632–636
31. Coppens P, Fournier B (2015) New methods in time-resolved Laue pump-probe crystallography at synchrotron sources. J Synchrotron Radiat 22:280–287
32. Bourgeois D, Wagner U, Wulff M (2000) Towards automated Laue data processing: application to the choice of optimal X-ray spectrum. Acta Crystallogr D Struct Biol 56:973–985
33. Coppens P, Vorontsov II, Graber T, Gembicky M, Kovalevsky AY (2005) The structure of short-lived excited states of molecular complexes by time-resolved X-ray diffraction. Acta Crystallogr A 61:162–172
34. Benedict JB, Makal A, Sokolow JD, Trzop E, Scheins S, Henning R, Graber T, Coppens P (2011) Time-resolved Laue diffraction of excited species at atomic resolution: 100 ps single-pulse diffraction of the excited state of the organometallic complex Rh-2(mu-PNP)(2)(PNP)(2) center dot BPh4. Chem Commun 47(6):1704–1706
35. Coppens P, Pitak M, Gembicky M, Messerschmidt M, Scheins S, Benedict J, Adachi S, Sato T, Nozawa S, Ichiyanagi K, Chollet M, Koshihara S (2009) The RATIO method for time-resolved Laue crystallography. J Synchrotron Radiat 16:226–230
36. Vorontsov I, Pillet S, Kaminski R, Schmokel MS, Coppens P (2010) LASER – a program for response-ratio refinement of time-resolved diffraction data. J Appl Cryst 43:1129–1130
37. Fournier B, Sokolow J, Coppens P (2016) Analysis of multicrystal pump-probe data sets. II Scaling of ratio data sets. Acta Crystallogr A Found Adv 72:250–260
38. Fournier B, Coppens P (2014) On the assessment of time-resolved diffraction results. Acta Crystallogr A Found Adv 70:291–299
39. Collet E, Moisan N, Balde C, Bertoni R, Trzop E, Laulhe C, Lorenc M, Servol M, Cailleau H, Tissot A, Boillot ML, Graber T, Henning R, Coppens P, Buron-Le Cointe M (2012) Ultrafast spin-state photoswitching in a crystal and slower consecutive processes investigated by femtosecond optical spectroscopy and picosecond X-ray diffraction. Phys Chem Chem Phys 14(18):6192–6199
40. Coppens P, Iversen B, Larsen FK (2005) The use of synchrotron radiation in X-ray charge density analysis of coordination complexes. Coord Chem Rev 249(1–2):179–195
41. Coppens P (2017) The dramatic development of X-ray photocrystallography over the past six decades. Struct Dyn 4(3)
42. Spence JCH (2017) X-ray lasers in biology: structure and dynamics. In: Hawkes PW (ed) Advances in imaging and electron physics, vol 200. Academic Press Inc, pp 103–152
43. Spence JCH (2017) XFELs for structure and dynamics in biology. Iucrj 4:322–339
44. Pande K, Hutchison CDM, Groenhof G, Aquila A, Robinson JS, Tenboer J, Basu S, Boutet S, DePonte DP, Liang MN, White TA, Zatsepin NA, Yefanov O, Morozov D, Oberthuer D, Gati C, Subramanian G, James D, Zhao Y, Koralek J, Brayshaw J, Kupitz C, Conrad C, Roy-Chowdhury S, Coe JD, Metz M, Xavier PL, Grant TD, Koglin JE, Ketawala G, Fromme R, Srajer V, Henning R, Spence JCH, Ourmazd A, Schwander P, Weierstall U, Frank M, Fromme P, Barty A, Chapman HN, Moffat K, van Thor JJ, Schmidt M (2016) Femtosecond structural dynamics drives the trans/cis isomerization in photoactive yellow protein. Science 352(6286):725–729
45. Chapman HN, Fromme P, Barty A, White TA, Kirian RA, Aquila A, Hunter MS, Schulz J, DePonte DP, Weierstall U, Doak RB, Maia F, Martin AV, Schlichting I, Lomb L, Coppola N, Shoeman RL, Epp SW, Hartmann R, Rolles D, Rudenko A, Foucar L, Kimmel N, Weidenspointner G, Holl P, Liang MN, Barthelmess M, Caleman C, Boutet S, Bogan MJ, Krzywinski J, Bostedt C, Bajt S, Gumprecht L, Rudek B, Erk B, Schmidt C, Homke A,

Reich C, Pietschner D, Struder L, Hauser G, Gorke H, Ullrich J, Herrmann S, Schaller G, Schopper F, Soltau H, Kuhnel KU, Messerschmidt M, Bozek JD, Hau-Riege SP, Frank M, Hampton CY, Sierra RG, Starodub D, Williams GJ, Hajdu J, Timneanu N, Seibert MM, Andreasson J, Rocker A, Jonsson O, Svenda M, Stern S, Nass K, Andritschke R, Schroter CD, Krasniqi F, Bott M, Schmidt KE, Wang XY, Grotjohann I, Holton JM, Barends TRM, Neutze R, Marchesini S, Fromme R, Schorb S, Rupp D, Adolph M, Gorkhover T, Andersson I, Hirsemann H, Potdevin G, Graafsma H, Nilsson B, Spence JCH (2011) Femtosecond X-ray protein nanocrystallography. Nature 470(7332):73–U81

46. Schmidt M, Pande K, Basu S, Tenboer J (2015) Room temperature structures beyond 1.5 angstrom by serial femtosecond crystallography. Struct Dyn 2(4)
47. Coppens P, Fournier B (2015) On the scaling of multicrystal data sets collected at high-intensity X-ray and electron sources. Struct Dyn 2(6)
48. Srajer V, Teng TY, Ursby T, Pradervand C, Ren Z, Adachi S, Schildkamp W, Bourgeois D, Wulff M, Moffat K (1996) Photolysis of the carbon monoxide complex of myoglobin: nanosecond time-resolved crystallography. Science 274(5293):1726–1729
49. Lim MH, Jackson TA, Anfinrud PA (1995) Midinfrared vibrational-spectrum of co after photodissociation from heme evidence for a ligand docking site in the heme pocket of hemoglobin and myoglobin. J Chem Phys 102(11):4355–4366
50. Lim M, Jackson TA, Anfinrud PA (1995) Binding of co to myoglobin from a heme pocket docking site to form nearly linear FE-C-O. Science 269(5226):962–966
51. Franzen S, Bohn B, Poyart C, Martin JL (1995) Evidence for subpicosecond heme doming in hemoglobin and myoglobin – a time-resolved resonance Raman comparison of carbonmonoxy and deoxy species. Biochemistry 34(4):1224–1237
52. Srajer V, Ren Z, Teng TY, Schmidt M, Ursby T, Bourgeois D, Pradervand C, Schildkamp W, Wulff M, Moffat K (2001) Protein conformational relaxation and ligand migration in myoglobin: a nanosecond to millisecond molecular movie from time-resolved Laue X-ray diffraction. Biochemistry 40(46):13802–13815
53. Jung YO, Lee JH, Kim J, Schmidt M, Moffat K, Šrajer V, Ihee H (2013) Volume-conserving trans–cis isomerization pathways in photoactive yellow protein visualized by picosecond X-ray crystallography. Nat Chem 5(3):212–220
54. Schotte F, Cho HS, Kaila VRI, Kamikubo H, Dashdorj N, Henry ER, Graber TJ, Henning R, Wulff M, Hummer G, Kataoka M, Anfinrud PA (2012) Watching a signaling protein function in real time via 100-ps time-resolved Laue crystallography. Proc Natl Acad Sci 109 (47):19256–19261
55. Ren Z, Perman B, Šrajer V, Teng TY, Pradervand C, Bourgeois D, Schotte F, Ursby T, Kort R, Wulff M, Moffat K (2001) A molecular movie at 1.8 Å resolution displays the photocycle of photoactive yellow protein, a eubacterial blue-light receptor, from nanoseconds to seconds. Biochemistry 40(46):13788–13801
56. Helliwell JR, Mitchell EP (2015) Synchrotron radiation macromolecular crystallography: science and spin-offs. Iucrj 2:283–291
57. Moffat K (2014) Time-resolved crystallography and protein design: signalling photoreceptors and optogenetics. Philos Trans R Soc B Biol Sci 369(1647):20130568
58. Moffat K (2001) Time-resolved biochemical crystallography: a mechanistic perspective. Chem Rev 101(6):1569–1581
59. Schmidt M (2019) Time-resolved macromolecular crystallography at pulsed X-ray sources. Int J Mol Sci 20(6)
60. Nam KH (2019) Sample delivery Media for Serial Crystallography. Int J Mol Sci 20(5)
61. Chapman HN (2019) X-ray free-electron lasers for the structure and dynamics of macromolecules. In: Kornberg RD (ed) Annual review of biochemistry, vol 88. Annual Reviews, pp 35–58
62. Srajer V, Schmidt M (2017) Watching proteins function with time-resolved x-ray crystallography. J Phys D Appl Phys 50(37)
63. Johansson LC, Stauch B, Ishchenko A, Cherezov V (2017) A bright future for serial femtosecond crystallography with XFELs. Trends Biochem Sci 42(9):749–762

64. Jaeger K, Dworkowski F, Nogly P, Milne C, Wang M, Standfuss J (2016) Serial millisecond crystallography of membrane proteins. In: Moraes I (ed) Next generation in membrane protein structure determination. Advances in experimental medicine and biology, vol 922, pp 137–149
65. Dickerson JL, McCubbin PTN, Garman EF (2020) RADDOSE-XFEL: femtosecond time-resolved dose estimates for macromolecular X-ray free-electron laser experiments. J Appl Cryst 53:549–560
66. de la Mora E, Coquelle N, Bury CS, Rosenthal M, Holton JM, Carmichael I, Garman EF, Burghammer M, Colletier JP, Weik M (2020) Radiation damage and dose limits in serial synchrotron crystallography at cryo- and room temperatures. Proc Natl Acad Sci U S A 117 (8):4142–4151
67. Garman EF, Weik M (2019) X-ray radiation damage to biological samples: recent progress. J Synchrotron Radiat 26:907–911
68. Lee D, Park S, Lee K, Kim J, Park G, Nam KH, Baek S, Chung WK, Lee JL, Cho Y, Park J (2020) Application of a high-throughput microcrystal delivery system to serial femtosecond crystallography. J Appl Cryst 53:477–485
69. Cohen MD, Schmidt GMJ, Sonntag FI (1964) Topochemistry. Part 2. Photochemistry of trans-cinnamic acids. J Chem Soc:2000
70. Cohen MD, Schmidt GMJ, Flavian S (1964) Topochemistry. Part 6. Experiments on photochromy + thermochromy of crystalline anils of salicylaldehydes. J Chem Soc:2041
71. Cohen MD, Schmidt GMJ (1964) Topochemistry. Part 1. Survey. J Chem Soc:1996
72. Cohen MD (1975) The photochemistry of organic solids. Angew Chem Int Ed Engl 14 (6):386–393
73. Natarajan A, Bhogala BR (2011) Bimolecular photoreactions in the crystalline state. Wiley, Hoboken, pp 175–228
74. Jarvis AG, Sparkes HA, Tallentire SE, Hatcher LE, Warren MR, Raithby PR, Allan DR, Whitwood AC, Cockett MCR, Duckett SB, Clark JL, Fairlamb IJS (2012) Photochemical-mediated solid-state 2+2 -cycloaddition reactions of an unsymmetrical dibenzylidene acetone (monothiophos-dba). CrstEngComm 14(17):5564–5571
75. Cao DK, Sreevidya TV, Botoshansky M, Golden G, Benedict JB, Kaftory M (2010) Kinetics of solid state photodimerization of 1,4-dimethyl-2-pyridinone in its molecular compound. J Phys Chem A 114(27):7377–7381
76. Benedict JB, Coppens P (2009) Kinetics of the single-crystal to single-crystal two-photon photodimerization of alpha-trans-cinnamic acid to alpha-truxillic acid. J Phys Chem A 113 (13):3116–3120
77. Zhang JJ, Zou Q, Tian H (2013) Photochromic materials: more than meets the eye. Adv Mater 25(3):378–399
78. Cole JM (2011) A new form of analytical chemistry: distinguishing the molecular structure of photo-induced states from ground-states. Analyst 136(3):448–455
79. Manrique-Juarez MD, Rat S, Salmon L, Molnar G, Quintero CM, Nicu L, Shepherd HJ, Bousseksou A (2016) Switchable molecule-based materials for micro- and nanoscale actuating applications: achievements and prospects. Coord Chem Rev 308:395–408
80. Gural'skiy IA, Quintero CM, Costa JS, Demont P, Molnar G, Salmon L, Shepherd HJ, Bousseksou A (2014) Spin crossover composite materials for electrothermomechanical actuators. J Mater Chem C 2(16):2949–2955
81. Shepherd HJ, Gural'skiy IA, Quintero CM, Tricard S, Salmon L, Molnár G, Bousseksou A (2013) Molecular actuators driven by cooperative spin-state switching. Nat Commun 4 (1):2607
82. Coppens P, Gerlits O, Vorontsov II, Kovalevsky AY, Chen YS, Graber T, Gembicky M, Novozhilova IV (2004) A very large Rh-Rh bond shortening on excitation of the [Rh-2 (1,8-diisocyano-p-menthane)(4)](2+) ion by time-resolved synchrotron X-ray diffraction. Chem Commun 19:2144–2145
83. Kim CD, Pillet S, Wu G, Fullagar WK, Coppens P (2002) Excited-state structure by time-resolved X-ray diffraction. Acta Crystallogr A 58:133–137

84. Schaniel D, Casaretto N, Bendeif E, Woike T, Gallien AKE, Klufers P, Kutniewska SE, Kaminski R, Bouchez G, Boukheddaden K, Pillet S (2019) Evidence for a photoinduced isonitrosyl isomer in ruthenium dinitrosyl compounds. CrstEngComm 21(38):5804–5810
85. Cole JM, Velazquez-Garcia JJ, Gosztola DJ, Wang SG, Chen Y-S (2018) η2-SO2 linkage photoisomer of an osmium coordination complex. Inorg Chem 57(5):2673–2677
86. Cole JM (2004) Single-crystal X-ray diffraction studies of photo-induced molecular species. Chem Soc Rev 33(8):501–513
87. Coppens P, Novozhilova I, Kovalevsky A (2002) Photoinduced linkage isomers of transition-metal nitrosyl compounds and related complexes. Chem Rev 102(4):861–883
88. Cormary B, Ladeira S, Jacob K, Lacroix PG, Woike T, Schaniel D, Malfant I (2012) Structural influence on the photochromic response of a series of ruthenium mononitrosyl complexes. Inorg Chem 51(14):7492–7501
89. Zangl A, Klufers P, Schaniel D, Woike T (2009) Photoinduced linkage isomerism of binuclear bis(pyrazole-3,5-dicarboxylato)-bridged {RuNO}(6) centres. Inorg Chem Commun 12 (10):1064–1066
90. Dieckmann V, Eicke S, Rack JJ, Woike T, Imlau M (2009) Pronounced photosensitivity of molecular Ru(bpy)(2)(OSO) (+) solutions based on two photoinduced linkage isomers. Opt Express 17(17):15052–15060
91. Schaniel D, Bendeif EE, Woike T, Bottcher HC, Pillet S (2018) Wavelength-selective photoisomerisation of nitric oxide and nitrite in a rhodium complex. CrstEngComm 20 (44):7100–7108
92. Galle G, Nicoul M, Woike T, Schaniel D, Freysz E (2012) Unraveling the mechanism of NO ligand photoisomerism by time-resolved infrared spectroscopy. Chem Phys Lett 552:64–68
93. Schaniel D, Woike T (2009) Necessary conditions for the photogeneration of nitrosyl linkage isomers. Phys Chem Chem Phys 11(21):4391–4395
94. Coppens P, Zheng SL, Gembicky M (2008) Static and time-resolved photocrystallographic studies in supramolecular solids. Z Kristall 223(4–5):265–271
95. Phillips AE, Cole JM, d'Almeida T, Low KS (2012) Ru–OSO coordination Photogenerated at 100 K in Tetraammineaqua(sulfur dioxide)ruthenium(II) (±)-Camphorsulfonate. Inorg Chem 51(3):1204–1206
96. Hatcher LE (2016) Raising the (metastable) bar: 100% photo-switching in [Pd(Bu4dien)(η1-O2)]+ approaches ambient temperature. CrstEngComm 18(22):4180–4187
97. Ohashi Y, Yanagi K, Kurihara T, Sasada Y, Ohgo Y (1981) Crystalline state reaction of cobaloxime complexes by x-ray exposure. 1. Direct observation of cobalt-carbon bond cleavage in [(R)-1-cyanoethyl][(S)-(−)-.alpha.-methylbenzylamine]bis(dimethylglyoximato)-cobalt(III). J Am Chem Soc 103(19):5805–5812
98. Decurtins S, Gutlich P, Kohler CP, Spiering H, Hauser A (1984) Light-induced excited spin STATE trapping in a transition-metal complex – the hexa-1-propyltetrazole-iron (II) tetrafluoroborate-crossover system. Chem Phys Lett 105(1):1–4
99. Carbonera C, Costa JS, Money VA, Elhaik J, Howard JAK, Halcrow MA, Letard JF (2006) Photomagnetic properties of iron(II) spin crossover complexes of 2,6-dipyrazolylpyridine and 2,6-dipyrazolylpyrazine ligands. Dalton Trans 25:3058–3066
100. Thompson AL, Money VA, Goeta AE, Howard JAK (2005) Structural studies of thermal- and light-induced transitions in iron(II) spin-crossover complexes. C R Chim 8(9–10):1365–1373
101. Money VA, Evans IR, Elhaik J, Halcrow MA, Howard JAK (2004) An X-ray powder diffraction study of the spin-crossover transition and structure of bis (2,6-dipyrazol-1-ylpyrazine)iron(II) perchlorate. Acta Crystallogr B Struct Sci Cryst Eng Mater 60:41–45
102. Money VA, Elhaik J, Halcrow MA, Howard JAK (2004) The thermal and light induced spin transition in FeL2 (BF4)(2) (L=2,6-dipyrazol-1-yl-4-hydroxymethylpyridine). Dalton Trans 10:1516–1518
103. Money VA, Elhaik J, Evans IR, Halcrow MA, Howard JAK (2004) A study of the thermal and light induced spin transition in FeL2 (BF4)(2) and FeL2 (ClO4)(2) L=2,6-di(3-methylpyrazol-1-yl)pyrazine. Dalton Trans 1:65–69

104. Money VA, Costa JS, Marcen S, Chastanet G, Elhaik J, Halcrow MA, Howard JAK, Letard JF (2004) A photomagnetic study of three iron(II) compounds containing ligands from the 2,6-di (pyrazol-1-yl)pyridine series. Chem Phys Lett 391(4–6):273–277
105. Letard JF, Guionneau P, Rabardel L, Howard JAK, Goeta AE, Chasseau D, Kahn O (1998) Structural, magnetic, and photomagnetic studies of a mononuclear iron(II) derivative exhibiting an exceptionally abrupt spin transition. Light-induced thermal hysteresis phenomenon. Inorg Chem 37(17):4432–4441
106. Gutlich P, Gaspar AB, Garcia Y (2013) Spin state switching in iron coordination compounds. Beilstein J Org Chem 9:342–391
107. Halcrow MA (2008) Trapping and manipulating excited spin states of transition metal compounds. Chem Soc Rev 37(2):278–289
108. Techert S, Schotte F, Wulff M (2001) Picosecond x-ray diffraction probed transient structural changes in organic solids. Phys Rev Lett 86(10):2030–2033
109. Rice SF, Gray HB (1983) Electronic absorption and emission spectra of binuclear platinum (II) complexes. Characterization of the lowest singlet and triplet excited states of tetrakis (diphosphonato)diplatinate(4-) anion (Pt2(H2P2O5)44-). J Am Chem Soc 105(14):4571–4575
110. Leung KH, Phillips DL, Che CM, Miskowski VM (1999) Resonance Raman intensity analysis investigation of metal-metal bonded transitions: an examination of the (1)A(2u) <– (1)A (1g) (5d sigma* -> 6p sigma) transition of Pt-2(P2O5H2)(4)(4-). J Raman Spectrosc 30 (11):987–993
111. Thiel DJ, Liviņs P, Stern EA, Lewis A (1993) Microsecond-resolved XAFS of the triplet excited state of Pt2(P2O5H2)4(4-). Nature 362(6415):40–43
112. Ozawa Y, Terashima M, Mitsumi M, Toriumi K, Yasuda N, Uekusa H, Ohashi Y (2003) Photoexcited crystallography of diplatinum complex by multiple-exposure IP method. Chem Lett 32(1):62–63
113. Christensen M, Haldrup K, Bechgaard K, Feidenhans'l R, Kong QY, Cammarata M, Lo Russo M, Wulff M, Harrit N, Nielsen MM (2009) Time-resolved X-ray scattering of an electronically excited state in solution. Structure of the (3)A(2u) state of Tetrakis-mu-pyrophosphitodiplatinate(II). J Am Chem Soc 131(2):502–508
114. van der Veen RM, Milne CJ, Pham VT, El Nahhas A, Weinstein JA, Best J, Borca CN, Bressler C, Chergui M (2008) EXAFS structural determination of the Pt-2(P2O5H2)(4)(4-) anion in solution. Chimia 62(4):287–290
115. Miskowski VM, Rice SF, Gray HB, Dallinger RF, Milder SJ, Hill MG, Exstrom CL, Mann KR (1994) Spectroscopy and photophysics of RH2(dimen)4(2+) (dimen = 1,8-diisocyanomenthane) – exceptional metal-metal bond shortening in the lowest electronic excited-states. Inorg Chem 33(13):2799–2807
116. Vorontsov II, Kovalevsky AY, Chen YS, Graber T, Gembicky M, Novozhilova IV, Omary MA, Coppens P (2005) Shedding light on the structure of a photoinduced transient excimer by time-resolved diffraction. Phys Rev Lett 94(19):4
117. Vorontsov II, Graber T, Kovalevsky AY, Novozhilova IV, Gembicky M, Chen YS, Coppens P (2009) Capturing and analyzing the excited-state structure of a Cu(I) phenanthroline complex by time-resolved diffraction and theoretical calculations. J Am Chem Soc 131(18):6566–6573
118. Ohashi Y (2013) Dynamic motion and various reaction paths of cobaloxime complexes in crystalline-state photoreaction. Crystallogr Rev 19(Suppl 1):2–146
119. Coppens P, Zheng SL, Gembicky M, Messerschmidt M, Dominiak PM (2006) Supramolecular solids and time-resolved diffraction. CrstEngComm 8(10):735–741
120. Zheng SL, Gembicky M, Messerschmidt M, Dominiak PM, Coppens P (2006) Effect of the environment on molecular properties: synthesis, structure, and photoluminescence of Cu(I) bis (2,9-dimethyl-1,10-phenanthroline) nanoclusters in eight different supramolecular frameworks. Inorg Chem 45(23):9281–9289
121. Zheng SL, Messerschmidt M, Coppens P (2005) An unstable ligand-unsupported Cu-I dimer stabilized in a supramolecular framework. Angew Chem Int Ed 44(29):4614–4617

122. Inokuma Y, Kawano M, Fujita M (2011) Crystalline molecular flasks. Nat Chem 3 (5):349–358
123. Kawano M, Fujita M (2007) Direct observation of crystalline-state guest exchange in coordination networks. Coord Chem Rev 251(21–24):2592–2605
124. Kawano M, Kobayashi Y, Ozeki T, Fujita M (2006) Direct crystallographic observation of a coordinatively unsaturated transition-metal complex in situ generated within a self-assembled cage. J Am Chem Soc 128(20):6558–6559
125. Haneda T, Kawano M, Kawamichi T, Fujita M (2008) Direct observation of the labile imine formation through single-crystal-to-single-crystal reactions in the pores of a porous coordination network. J Am Chem Soc 130(5):1578–1579
126. Kawamichi T, Haneda T, Kawano M, Fujita M (2009) X-ray observation of a transient hemiaminal trapped in a porous network. Nature 461(7264):633–635
127. Horiuchi S, Murase T, Fujita M (2011) Noncovalent trapping and stabilization of dinuclear ruthenium complexes within a coordination cage. J Am Chem Soc 133(32):12445–12447
128. Takezawa H, Murase T, Fujita M (2012) Temporary and permanent trapping of the metastable twisted conformer of an overcrowded chromic alkene via encapsulation. J Am Chem Soc 134 (42):17420–17423
129. Blake AJ, Champness NR, Easun TL, Allan DR, Nowell H, George MW, Jia J, Sun XZ (2010) Photoreactivity examined through incorporation in metal-organic frameworks. Nat Chem 2 (8):688–694
130. Easun TL, Jia JH, Reade TJ, Sun XZ, Davies ES, Blake AJ, George MW, Champness NR (2014) Modification of coordination networks through a photoinduced charge transfer process. Chem Sci 5(2):539–544
131. Makal A, Benedict J, Trzop E, Sokolow J, Fournier B, Chen Y, Kalinowski JA, Graber T, Henning R, Coppens P (2012) Restricted photochemistry in the molecular solid state: structural changes on photoexcitation of Cu(I) phenanthroline metal-to-ligand charge transfer (MLCT) complexes by time-resolved diffraction. J Phys Chem A 116(13):3359–3365
132. Kalinowski JA, Fournier B, Makal A, Coppens P (2012) The LaueUtil toolkit for Laue photocrystallography. II. Spot finding and integration. J Synchrotron Radiat 19:637–646
133. Kaminski R, Graber T, Benedict JB, Henning R, Chen YS, Scheins S, Messerschmidt M, Coppens P (2010) Optimizing the accuracy and precision of the single-pulse Laue technique for synchrotron photo-crystallography. J Synchrotron Radiat 17:479–485
134. Jarzembska KN, Kaminski R, Fournier B, Trzop E, Sokolow JD, Henning R, Chen Y, Coppens P (2014) Shedding light on the photochemistry of coinage-metal phosphorescent materials: a time-resolved Laue diffraction study of an Ag-I-Cu-I tetranuclear complex. Inorg Chem 53(19):10594–10601
135. Jarzembska KN, Hapka M, Kaminski R, Bury W, Kutniewska SE, Szarejko D, Szczesniak MM (2019) On the nature of luminescence thermochromism of multinuclear copper (I) benzoate complexes in the crystalline state. Crystals 9(1)
136. Collet E, Lorenc M, Cammarata M, Guérin L, Servol M, Tissot A, Boillot M-L, Cailleau H, Buron-Le Cointe M (2012) 100 picosecond diffraction catches structural transients of laser-pulse triggered switching in a spin-crossover crystal. Chemistry 18(7):2051–2055
137. Bertoni R, Cammarata M, Lorenc M, Matar SF, Létard J-F, Lemke HT, Collet E (2015) Ultrafast light-induced spin-state trapping photophysics investigated in Fe(phen)2(NCS)2 spin-crossover crystal. Acc Chem Res 48(3):774–781
138. Bertoni R, Lorenc M, Laisney J, Tissot A, Moreac A, Matar SF, Boillot ML, Collet E (2015) Femtosecond spin-state photo-switching dynamics in an Fe-III spin crossover solid accompanied by coherent structural vibrations. J Mater Chem C 3(30):7792–7801
139. Coppens P (2015) Perspective: on the relevance of slower-than-femtosecond time scales in chemical structural-dynamics studies. Struct Dyn 2(2)
140. Basuroy K, Chen Y, Sarkar S, Benedict J, Coppens P (2017) Exploring the structural changes on excitation of a luminescent organic bromine-substituted complex by in-house time-resolved pump-probe diffraction. Struct Dyn 4(2)